Metabolism of versicolorin A, a genotoxic precursor of aflatoxin B1: Characterization of metabolites using in vitro production of standards

Carine Al-Ayoubi, Justin Oules, Elodie Person, Sandrine S. Bruel, Alyssa Bouville, Philippe Pinton, Isabelle Oswald, Emilien Jamin, Olivier Puel, Laura Soler-Vasco

Metabolism of Versicolorin A, a genotoxic precursor of Aflatoxin B1: Characterization of metabolites using *in vitro* production of standards

Carine Al-Ayoubi[1*], Justin Oules[1,2*], Elodie Person[1], Sandrine Bruel[1], Alyssa Bouville[1,2], Philippe Pinton[1], Isabelle P. Oswald[1], Emilien L. Jamin[1,2,3], Olivier Puel[1] and Laura Soler[1]

[1] *Toxalim (Research Center in Food Toxicology), Université de Toulouse, INRAE, ENVT, INP-Purpan, Toulouse, France*

[2] *MetaboHUB-MetaToul, National Infrastructure of Metabolomics and Fluxomics, Toulouse, 31077 France*

[3] *France Exposome, INSERM INRAE INERIS ONIRIS Université Rennes 1 Université Paris Cité, Rennes, France*

**These authors contributed equally to this work*

Corresponding Author :

Emilien L. Jamin

INRAE, UMR-1331, Toxalim, 180 chemin de Tournefeuille, 31027 Toulouse cedex 3, France

Phone +33 82 06 63 93

E-Mail: Emilien.Jamin@inrae.fr

Abstract

The toxicity of mycotoxins containing bisfuranoid structures such as aflatoxin B1 (AFB1) depends largely on biotransformation processes. While the genotoxicity and mutagenicity of several bisfuranoid mycotoxins including AFB1 and sterigmatocystin have been linked to *in vivo* bioactivation of these molecules into reactive epoxide forms, the metabolites of genotoxic and mutagenic AFB1 precursor versicolorin A (VerA) have not yet been characterized. Because this molecule is not available commercially, our strategy was to produce a library of metabolites derived from the biotransformation of in-house purified VerA, following incubation with human liver S9 fractions, in presence of appropriate cofactors. The resulting chromatographic and mass-spectrometric data were used to identify VerA metabolites produced by intestinal cell lines as well as intestinal and liver tissues exposed *ex vivo*. In this way, we obtained a panel of metabolites suggesting the involvement of phase I (M + O) and phase II (glucuronide and sulfate metabolites) enzymes, the latter of which is implicated in the detoxification process. This first qualitative description of the metabolization products of VerA suggests bioactivation of the molecule into an epoxide form and provides qualitative analytic data to further conduct a precise metabolism study of VerA required for the risk assessment of this emerging mycotoxin.

Keywords: Versicolorin A, Aflatoxin B1, S9 fractions, Biomonitoring, Metabolites,

1. Introduction

Mycotoxins are widespread toxic secondary fungal metabolites that contaminate food and feed (Payros et al., 2021). Aflatoxins (AFs) are considered to be the most dangerous family of mycotoxins, while aflatoxin B1 (AFB1) is the most frequent and most toxic member of this family, and is the strongest known natural carcinogen (classified as Group 1 by IARC) (IARC, 1993; Schrenk et al., 2020). The presence of AFs in food and animal feed, in particular of AFB1, is regulated in most parts of the world (European Commission, 2006; US Food and Drugs Administration, 2021, 2019). In Europe, the maximum authorized levels of aflatoxins range from 0.1 to 15 µg/kg (European Union, 2006).

AF synthesis involves several enzymatic reactions and at least 15 compounds have been reported as intermediates of the aflatoxin biosynthetic pathway (Fig. 1; Caceres et al., 2020). Notably during the final steps of the synthesis of AFB1 and Aflatoxin G1 (AFG1) a characteristic dihydrobisfuran ring structure is formed, which is also present in three intermediate precursors: sterigmatocystin (STC), O-methyl sterigmatocystin (OMST) and versicolorin A (VerA; Fig.1). The mycotoxins containing this structure are known as bisfuranoids. This structure drives the toxicity of these molecules, since the compounds containing an unsaturated vinyl ether double bond of the terminal furan ring have been described as mutagens and liver carcinogens (Hendricks et al., 1980; Mori et al., 1986; Wong et al., 1977). The involvement of this specific structure in the toxicity of AFB1 is well characterized, and is determined by epoxidation of the vinyl ether double bond mainly by the action of several cytochrome P450 (CYP450) enzymes in exposed tissues which metabolise AFB1 into the highly reactive aflatoxin-8,9-*exo*-epoxide known as AFBO (Eaton et al., 2010; Smela et al., 2001). AFBO reacts with critical biological nucleophiles, such as proteins and DNA, and causes point mutations, chromosomal aberrations, and genetic damage (Eaton et al., 2010). The detoxification of AFBO is achieved by glutathione-S-transferases (GST). Depending on the relative importance of these biotransformation routes and the GST-dependent detoxification of AFBO, differences can be found in the susceptibility of tissues or species to developing cancer, liver being the most sensitive organ, and humans and pigs being more sensitive than rats or mice, respectively (Chu, 2003; Eaton et al., 2010).

Fig. 1. Aflatoxin biosynthetic pathway

Schematization of the main biosynthetic reactions leading to aflatoxins synthesis produced by *Aspergillus* species: *A.flavus* (B1, B2) and *A.parasiticus* (B1, B2, G1, G2) (Adapted from Trail et al. (1995)). The structure of dihydrobisfuran ring is circled and the double bonds are highlighted in red.

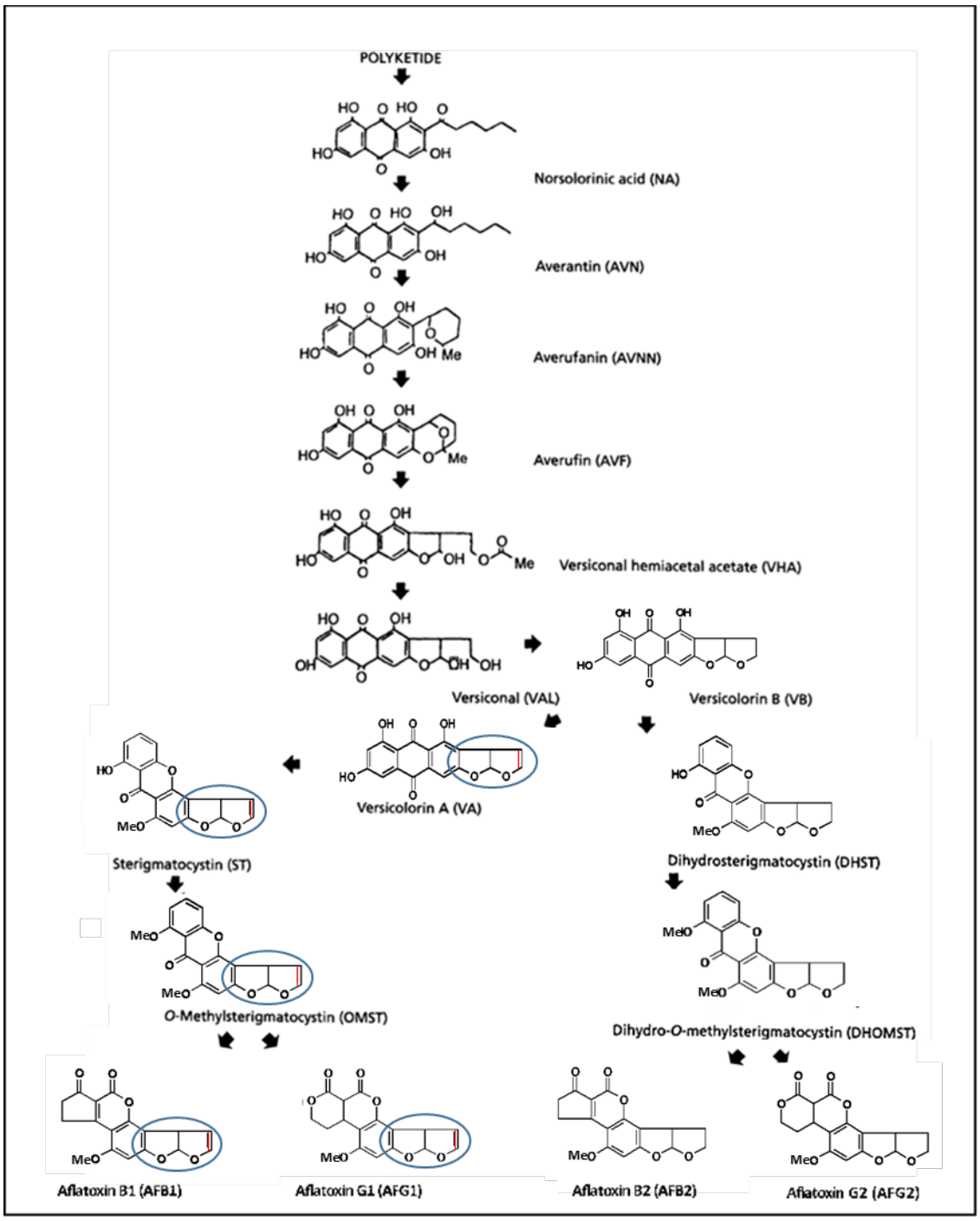

The biotransformation of other bisfuranoid AFB1 precursors has been less extensively investigated. The formation of reactive *exo*-epoxide forms of AFG1 and STC is described in the literature, along with their relationship with genotoxic effects (Baertschi et al., 1989; EFSA, 2013; Walkow et al., 1985). In the case of OMST, to our knowledge, no production of an epoxide form has been reported so far, and in fact, the genotoxicity of this compound is not established, as the results are contradictory. The distinctive methyl group present only in OMST may explain its apparently lower toxicity compared to other bisfuranoid mycotoxins (Mori et al., 1986; Theumer et al., 2018; Wehner et al., 1978). Hence, methylation of STC may be linked to a reduction in toxicity (Kawai et al., 1986). No data is available in the literature on the biotransformation of VerA or on its circulating concentrations in blood, even though this mycotoxin is highly genotoxic and mutagenic (Gauthier et al., 2020; Jakšić et al., 2012; Mori et al., 1986; Theumer et al., 2018).

VerA is considered to be an emerging threat, as it shows high *in vitro* cytotoxic, genotoxic and clastogenic potency in different cell lines, in some cases, even higher than AFB1 (Gauthier et al., 2020; Jakšić et al., 2012; Mori et al., 1986; Theumer et al., 2018). The characterization of the biotransformation of VerA is thus indispensable for a complete assessment of the risk, as indicated in a report published in 2017 by the joint FAO/WHO Expert Committee on Food Additives (JECFA; JECFA, 2017), which underlined the importance of producing sound data on the emerging threats represented by AF precursors. Moreover, metabolites derived from VerA would also need to be characterized to monitor the toxicokinetics of the molecule *in vivo* and to estimate actual exposure to VerA.

Biotransformation studies are usually conducted using radiolabeled compounds to allow their specific detection and quantification, followed by mass spectrometry to enable their identification (Jacques et al., 2010). However, this approach depends on the commercial availability of the radiolabeled standard, and is not easy to apply due to the complexity involved in handling radiolabeled compounds (Staack and Hopfgartner, 2007). Another possible solution is to analyze only using liquid chromatography combined with high-resolution mass spectrometry (HPLC-HRMS) (Fæste et al., 2011), but this approach requires validation of all each identification using metabolite standards, which are rarely commercially available. To get round the lack of standards, an approach aimed at *in vitro* production of

metabolites using human liver S9 fraction incubations was recently proposed for human biomonitoring (Huber et al., 2021). This method provides relevant data, such as MS spectra, MS/MS spectra and chromatographic retention times of metabolites that can confirm their identification in more diluted and complex samples. We previously applied this kind of structural validation of phase I and II metabolites in human urine samples during an exposome study, but using *in vivo* experiments (Jamin et al., 2014). Because VerA is not commercially available, human liver S9 fractions containing both microsomal and cytosolic enzymes were incubated with appropriate cofactors to explore the metabolic fate of VerA, to provide a comprehensive list of metabolites produced *in vitro,* and to elucidate major metabolite structures. In a second step, we obtained a broader overview of the metabolites possibly present in more complex samples using intestinal porcine epithelial cell line (IPEC1), porcine jejunum explants, and precision-cut liver slices exposed to VerA. Based on this workflow, we provide a first qualitative characterization of the metabolites derived from the metabolization of VerA. The list comprises degradation products, as well as phase I and phase II metabolites, including a metabolite compatible with possible bioactivation of VerA.

2. Material and Methods

2.1. Chemicals and reagents

HPLC grade solvents (methanol, acetonitrile), acetic acid, dichloromethane and chloroform were purchased from Fisher Scientific (Illkirch, France). Dulbecco′s Modified Eagle Medium/Nutrient Mixture F-12 Ham (DMEM/HAMs F12 medium), William's E Medium, phosphate buffered saline (PBS), insulin transferrin-selenium (ITS), alanine, dexamethasone, ethanol, DMSO, monobasic sodium phosphate, dibasic heptahydrate sodium phosphate, NADP, glucose, D-glucose 6-phosphate sodium salt, glucose-6-phosphate dehydrogenase, magnesium chloride ($MgCl_2$), reduced L-glutathione (GSH), sodium chloride (NaCl), 3′-phosphoadenosine-5′-phosphosulfate (PAPS), uridine 5′-diphosphoglucuronic acid (UDPGA), Krebs-Henseleit buffer (KHB), calcium chloride dihydrate ($CaCl_2$, $2H_2O$) and sodium bicarbonate ($NaHCO_3$) were purchased from Sigma-Aldrich Merck (Saint Quentin Fallavier, France). Streptomycin/penicillin, L-glutamine, fetal bovine serum (FBS) and gentamycin were purchased from Eurobio (Courtaboeuf, France). Epidermal growth factor (EGF) was

purchased from Becton-Dickinson (Le Pont de Claix, France). Alamethicin was purchased from Cayman Chemical (Ann Arbor, MI, USA). Ultrapure water was generated by a Milli-Q system (Millipore, Saint Quentin en Yvelines, France) with a specific resistance of 18.2 MΩ at 25 °C and total organic carbon (TOC) value < 3 ppb.

2.2. Purification of VerA

As VerA is not available commercially, it was purified using a previously described in-house protocol (Gauthier et al., 2020) from wheat grains colonized by a pathway-blocked strain of *Aspergillus parasiticus* that specifically accumulates VerA (*A. parasiticus* strain SRRC 0164). Briefly, VerA was extracted from wheat and mycelia in chloroform and then purified by high-performance liquid chromatography (HPLC) using an Ultimate 3000 HPLC system (Thermo Fisher Scientific, Courtaboeuf, France). An authentic VerA standard previously produced in our lab and checked by high resolution mass spectrometry (HRMS) and nuclear magnetic resonance analysis (NMR) was used as reference for both purification and to check purity (Theumer et al., 2018). The identity and purity of the purified VerA were confirmed by HPLC with a diode-array detector (DAD), following the protocol already used by our team and detailed in Theumer et al. (2018). The concentration of VerA produced was determined by reading absorbance at 290 nm ($\varepsilon_{25°C\ EtOH}$= 25,825) and 450 nm ($\varepsilon_{25°C\ EtOH}$=7,585) (Cole and Cox, 1981). Stock solution of VerA (10 mM) was prepared in DMSO and stored at -20 °C until use.

2.3. Incubation of VerA with human liver S9

Reference metabolites of VerA were produced *in vitro* using the S9 liver fraction, containing both phase I and phase II xenobiotic metabolizing enzymes (XME). Mixed-gender human liver S9 (pool comprising 50 donors) was purchased from Tebu-bio (Le Perray-en-Yvelines, France). The incubation method was adapted from previous studies (Cabaton et al., 2008; Jaeg et al., 2004). S9 incubations were prepared in a final volume of 0.5 mL of 0.1 M sodium/phosphate buffer pH 7.4 with 5 mM $MgCl_2$, with a protein content fixed at 6 mg/mL and with appropriate cofactors. A 15-min pre-incubation was performed with alamethicin (50 µg/mg protein, 0.15 mM in DMSO, 0.5% in the final volume) (pore-forming agent). Incubations were started with the addition of 50 µM VerA (0.6% ethanol in the final volume), GSH 12.5

mM, UDPGA 2 mM, PAPS 0.2 mM and a NADPH generating system consisting of NADP 1.3 mM, glucose-6-phosphate 5 mM and glucose-6-phosphate dehydrogenase 2 IU/mL. S9, VerA and cofactors were incubated for 3 h at 37 °C under shaking. Incubations were quenched with 1.5 mL acetonitrile, kept for 30 min on ice and centrifuged for 10 min at 6,500 *g* at 4 °C. Supernatants were collected, placed in HPLC vials and stored at -20 °C until HPLC-HRMS analyses. All the experiments were performed in triplicate. Control incubations were performed without VerA (proteins, cofactors and 0.6% ethanol) and with the addition of cofactors after the quenching step (proteins, VerA and cofactors), in order to distinguish non-cofactor-mediated VerA transformation and cofactor-dependant metabolites.

2.4 Exposure of cultured intestinal IPEC-1 cells to VerA

Cells were cultured in Petri dishes (100 x 20 mm; Cellstar, Greiner Bio-One, Germany) in DMEM/HAMs F12 medium, completed with 1% ITS, 1% streptomycin/penicillin, 1% L-glutamine, 5% FBS, and 5 µg/mL EGF. Cultures were kept under standardized conditions at 39 °C in a humidified atmosphere with 5% CO_2.

To mimic real conditions, prior to exposure, IPEC-1 cells were differentiated into monolayers. We chose to work at the same dose of VerA (50 µM) and time of exposure (3 h) as for *in vitro* S9 fraction experiments and to complete the study using an additional exposure condition of a less cytotoxic dose (10 µM) and longer exposure times (24 and 48 hours). IPEC-1 cells were differentiated as previously described (Pinton et al., 2009). Briefly, cells were plated at a density of 2.10^5 cells/mL in the aforementioned medium in permeable supports suitable for a 6-well plate with 0.4 µm polyethylene terephthalate membranes (Coring Falcon, Corning, NY, USA) until confluence was reached. The cells were then differentiated into monolayers in the same medium containing 20 µg/mL dexamethasone but without FBS until transepithelial electrical resistance stability was reached, which takes between 8 to 10 days. After washing with PBS, VerA was added on the apical side and incubated in the conditions described above. Control samples were treated with the vehicle (DMSO) in all cases.

187 At the end of the treatments, cells were scraped off using 0.9% cold isotonic NaCl solution, recovered
188 and centrifuged at 300 g for 10 minutes at 4 °C. After removal of the supernatant, the dry cell pellets
189 were stored at - 80 °C until further analysis.
190
191 2.5 Exposure of jejunum explants and precision-cut liver slices to VerA
192 Porcine tissues were used to evaluate VerA biotransformation in the intestine and liver. Jejunum
193 explants and precision-cut liver slices were prepared from four 35-day-old castrated male piglets.
194 Animal care and use for this study were carried out in accordance with the French Ministry of
195 Agriculture guidelines. All animal tissue procedures were performed in accordance with the ethics
196 Committee of Pharmacology-Toxicology of Toulouse-Midi-Pyrénées (APAFIS
197 #N2016080314392462). The dose of VerA (50 µM) and time of exposure (3 h) used in this study was
198 equivalent to that used for S9 fraction experiments.
199 The method of obtaining jejunum explants is described in detail in Lahjouji et al. (2020). Briefly, the
200 jejunum was rapidly extracted, flushed with phenol red-free William's E Medium completed with 1%
201 penicillin/streptomycin and 0.5% gentamycin, and opened longitudinally. A 6 mm diameter biopsy
202 punch was used to obtain jejunum explants that were placed with the mucosa facing upwards on sponges
203 in 6-well plates containing 3 mL medium (3 explants per well). Jejunum explants were then exposed for
204 3 h to 50 µM VerA or DMSO in William's E Medium supplemented with 25 g/L of glucose, 1% ITS,
205 1% alanine-glutamine, 1% penicillin/streptomycin and 0.5% gentamycin at 39 °C, and 5% CO_2-
206 controlled atmosphere with orbital shaking.
207 To prepare the liver slices (Hasuda et al., 2022), the liver was rapidly resected and the right lateral
208 hepatic lobe flushed with a 0.9% ice-cold isotonic NaCl solution to limit ischemia and remove
209 hemoglobin. To maintain explant viability, KHB supplemented with $NaHCO_3$ (2.1 g/L) and $CaCl_2$,
210 $2H_2O$ (0.373 g/L), previously bubbled with carbogen for 1 h, was used in the coring, slicing, and storage
211 procedures. After placing the perfused liver under a cylinder-shaped tissue coring tool (diameter 8 mm),
212 the tissue was drilled to make liver cores, and immediately placed in ice-cold buffer. Next, the cylindrical
213 cores were transferred to the holder of the Krumdieck tissue slicer (Alabama Research and
214 Development, AL, USA). Slices (250 µm thick) were prepared to optimize oxygen and nutrient intake

(De Graaf et al., 2010). Damaged slices were discarded. Before the slices were treated, a regeneration step was required, consisting of incubating the slices in William's E Medium supplemented with 1% glutamine and 0.5% gentamycin (2 mL per well) bubbled in carbogen for 1 h to enable homeostasis recovery. Liver slices were distributed in 12-well tissue culture plates (1 slice per well) using a spatula and exposed for 3 h to 50 µM VerA or DMSO in William's E Medium supplemented with 1% glutamine and 0.5% gentamycin (2 mL per well), at 37 °C under a 90% O_2 and 5% CO_2-controlled atmosphere. After the incubation period, the jejunum explants, liver slices, and their culture media were stored separately at -80 °C.

2.5 Extraction of metabolites from IPEC-1 cells, jejunum explants, and liver slices

Metabolites were extracted from IPEC-1 intestinal cell pellets by adding 1 mL of acetonitrile/ultrapure water (90:10 v/v) and vortexing for 1 min. This operation was repeated twice. After centrifugation at 5,340 g for 10 min, the supernatants were evaporated with a SpeedVac® (Thermo Scientific, Les Ulis, France) at ambient temperature. The extracts were finally dissolved in 250 µL of water/methanol/acetic acid (95:5:0.1 v/v/v).

Approximately 50 mg of tissue was weighed and placed in a 2 mL lysing matrix S tube (Fisher Scientific, Illkirch, France) for jejunum explants, or a 2 mL lysing matrix M tube (Fisher Scientific, Illkirch, France) for liver slices. Cold methanol was added to each tissue at a concentration of 4 mL/g, and cold water at 0.85 mL/g of tissue. Tissues were homogenized using a FastPrep® System (MP Biomedicals, Illkirch, France) to extract the metabolites. Jejunum explants were homogenized twice for 30 sec. at a speed of 6 a.u. (arbitrary units). Liver slices were homogenized for 40 sec. at a speed of 6 a.u. A volume of 2 mL/g of tissue of dichloromethane was added and the extracts were vortexed, followed by a second addition of 2 mL/g of tissue of dichloromethane and 2 mL/g of tissue of water. Samples were centrifuged at 2,870 g for 15 min at 4 °C. The lipid supernatant was removed and the aqueous phase was evaporated in a SpeedVac® (Thermo Scientific, Les Ulis, France). Finally, the extracts were suspended with 500 µL of water/methanol/acetic acid (95:5:0.1 v/v/v).

2.6 HPLC-HRMS analyses

Samples were analyzed with an RSLC 3000 HPLC system (Thermo Scientific, Les Ulis, France) coupled with an LTQ-Orbitrap XL mass spectrometer (Thermo Scientific, Les Ulis, France) equipped with a heated electrospray ionization source (HESI). A volume of 10 µL was injected onto a Hypersil Gold C18 column (100 x 2.1 mm, 1.9 µm; Thermo Fisher Scientific, Les Ulis, France) maintained at 40 °C. Analytical mobile phases were composed of water/methanol/acetic acid (95:5:0.1 v/v/v) for phase A and methanol/acetic acid (100:0.1 v/v) for phase B. Chromatographic separation was performed at a flow rate of 0.3 mL/min with the following gradient: 0% to 100% of B from 0 to 30 min, 100% of B from 30 min to 34 min. HRMS detection was performed between *m/z* 80 and 1,500 at a resolution of 30,000 (at *m/z* 400). For the positive ionization mode, the following HESI settings were applied: capillary temperature 300 °C, vaporizer temperature 400 °C, source voltage 4 kV, sheath gas (N_2) flow rate 30 a.u., auxiliary gas (N_2) flow rate 10 a.u. and tube lens offset 80 V. For the negative ionization mode, the following parameters were used: capillary temperature 300 °C, vaporizer temperature 400 °C, source voltage 2 kV, sheath gas (N_2) flow rate 40 a.u., auxiliary gas (N_2) flow rate 5 a.u. and tube lens offset -70 V. The high-resolution mass analyzer was calibrated in each ionization mode with calibration mixtures (Thermo Scientific, Les Ulis, France) based on the supplier's protocols, which allowed *m/z* measurements at ±5ppm**.**

A list of potential metabolites including hydroxylated, hydrolyzed, demethylated, conjugation with glucuronic acid or sulfate, was produced. Suspected metabolites were monitored using Xcalibur® (Thermo Scientific, Les Ulis, France) according to their exact mass with a window of +/- 5 ppm. A complementary screening step was performed using MetaSense software® (ACD/Labs, Strasbourg, France) to identify unexpected metabolites. When a potential metabolite was detected according to its *m/z* in extracts, and not in blank samples, targeted MS/MS and MS^3 experiments with the collision induced dissociation (CID) mode at a low resolution, or at a resolution of 7500 were triggered with a normalized collision energy of 25%. Identification nomenclature was based on the nomenclature of the metabolomics standards initiative (Sumner et al., 2007). The results were interpreted by looking at characteristic fragmentation patterns, assisted when necessary using CFM-ID (Allen et al., 2014).

3 Results

3.1 Construction of a library of VerA metabolites using the *in vitro* S9 fraction

VerA was first incubated with human liver S9 fractions combined with different cofactors to biosynthesize phase I and II metabolites. Six compounds were detected in negative mode ionization along with intact VerA (Table 1). Their *m/z* ratio was measured by HRMS with an error < 5 ppm, confirming their molecular formulae according to the technical specificities of the mass analyzer. Their product ions observed by MS/MS enabled us to propose an identification level for each compound (Sumner et al., 2007). Their structures are displayed in Figure 2. Positive ionization mode data are available in supplementary table 1. No metabolites were detected in control incubations. Unmodified VerA was detected in S9 fraction incubations and identification confirmed by a control. Phase I metabolites displayed a similar fragmentation pattern to that of VerA (i.e. mainly losses of CO, CO_2 as indicated in Table 1), but with *m/z* shifts in fragment ions in agreement with modifications in their chemical structure and with additional loss of water. Phase II metabolites showed characteristic fragment ions (Table 1) of glucuronic acid and sulfate groups with a loss of 176 u and 80 u, respectively (Jamin et al., 2014). Conjugated metabolites were confirmed by MS^3 experiments, displaying a similar fragmentation pattern as the non-conjugated molecule (see supplementary table 2).

The case of the M + O metabolite is particular since its chemical formula could correspond to different kind of structures. As illustrated in the Figure 3 with the well-studied AFB1, the 8,9-epoxide metabolite or hydroxylated metabolite (AFM1) displayed the same chemical formula, which correspond to the addition of one oxygen atom to the structure of the parent molecule. Therefore, it is not possible to differentiate the hydroxylated metabolite from the epoxide one only by the mass measurement. These isomer structures could potentially displayed different chromatographic retention times, but in our analytical conditions only one peak was detected, which can correspond to one or several co-eluted M + O metabolites (i.e. hydroxylated or epoxide). Furthermore, these similar structures are expected to produced similar fragment ions by low energy CID in MS/MS experiments according to *in silico*

fragmentation tools as CFM-ID. Thus, none of the detected fragment ions of M + O were specific of one hydroxylated or epoxide structure. Since VerA has asymmetric carbon atoms, diastereoisomers of epoxide metabolites are possible (known as endo or exo epoxide for AFB1) and could potentially be differentiated by MS/MS or chromatography. However, it was not more possible to differentiate them in our experimental conditions, than it was for hydoxylated metabolites.

Fig. 2. Identified structures of VerA metabolites

Highlighted atoms correspond to possible bonding positions. Red positions correspond to hydroxylation (-OH), green to conjugation with sulfate ($-SO_3$), blue to conjugation with glucuronic acid, grey to methylation ($-CH_3$), and pink to double bond reduction. Question marks indicate the uncertain biotransformation of VerA into an epoxide and/or hydroxylated form.

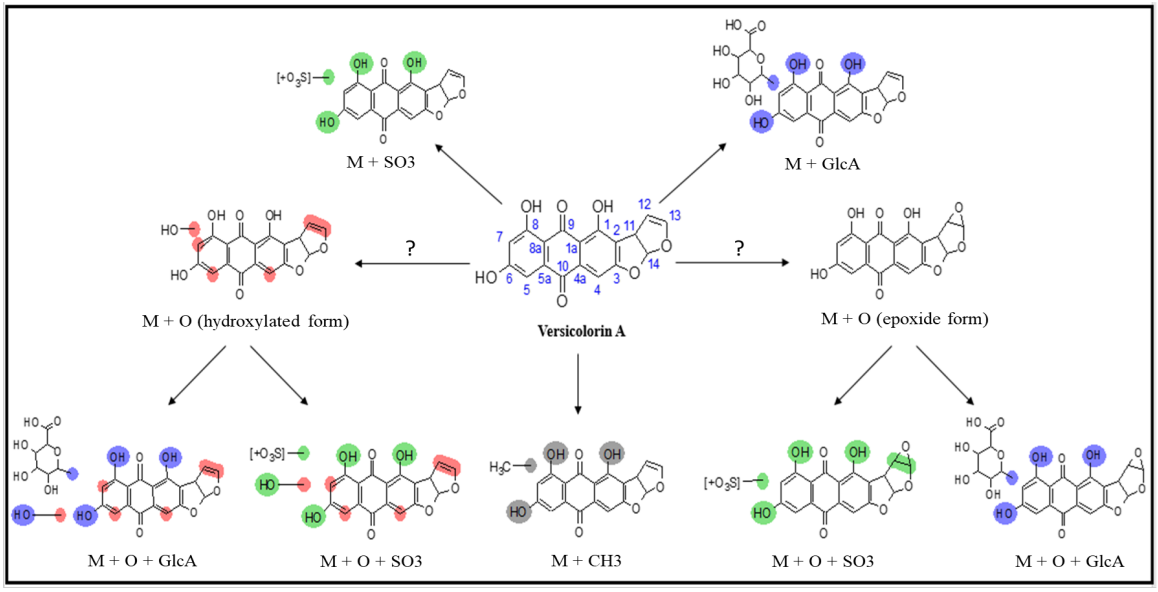

Table 1: Compounds detected as $[M-H]^-$ after VerA incubations with human liver S9, according to their measured *m/z* corresponding to the expected molecular formula with an *m/z* error below 5ppm. Observed chromatographic retention times are expressed in minutes, and detected MS/MS fragment ions are reported with their relative abundance.

Compound	Measured *m/z*	Error (ppm)	Molecular formula	Retention time (min)	Identification level[a]	MS/MS spectrum Observed product ions *m/z* (relative

						abundance expressed in %)
VerA	337.0359	-2.1	$C_{18}H_{10}O_7$	23.2	1	309.1 (100), 308.1 (55), 293.1 (14), 337.1 (12), 320.0 (5), 265 (5), 252 (4), 280 (3)
M + O ***epoxide and/or hydroxylated***	353.0304	-2.8	$C_{18}H_{10}O_8$	18.9	3	309.1 (100), 335.2 (97),325.1 (93), 281.1 (23), 310.1 (17), 265.1 (11), 297.1 (10), 307.1 (5), 308.0 (5), 311.1 (3), 324,2 (3), 353.0 (2)
M + H_2O	355.0465	1.7	$C_{18}H_{12}O_8$	18.4	3	337.1 (100), 309.1 (60), 310.1 (24), 327.1 (21), 355.2 (14), 299.1 (13), 325.1 (9), 311.1 (6), 293.2 (5), 284.0 (5), 297.2 (4), 270.1 (3)
M + GlcAc	513.0677	2.7	$C_{24}H_{18}O_{13}$	19.1	3	337.1 (100), 175.0 (2), 51.3.1 (2)
M + O + GlcAc ***epoxide and/or hydrohylated***	529.0619	-2.1	$C_{24}H_{18}O_{14}$	14.2	3	353.1 (100), 529.1 (2)
M + SO_3	416.9910	-2.9	$C_{18}H_{10}O_{10}S$	22.0	3	337.1 (100), 417.0 (2)
M + O + SO_3 ***epoxide and/or hydroxylated***	432.9859	-2.8	$C_{18}H_{10}O_{11}S$	14.9	3	353.1 (100),433.0 (2)

313 [a] Identification level as defined by Sumner et al., 2007

314 **Figure 3: structures of the known epoxide and hydroxylated (AFM1) metabolites of AFB1.**

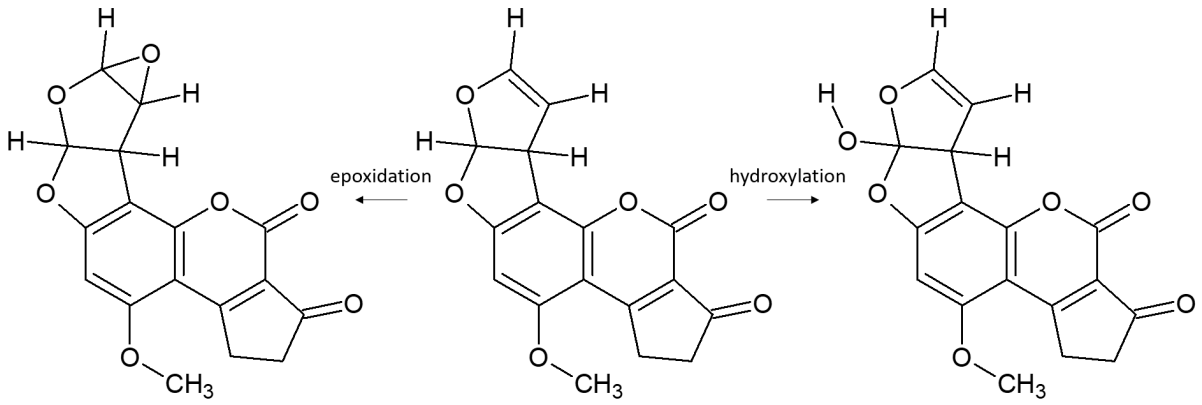

3.2 VerA metabolites identified in IPEC-1 intestinal epithelial cells

To obtain a first overview of VerA metabolites that could be produced in the intestine, cultured intestinal IPEC-1 cells were exposed to VerA. Although the amount of material obtained using cultured cells is limited, the use of a biological sample of intermediate complexity compared to tissues helped interpret the results as a whole. Metabolites were characterized according to the chromatographic, MS and MS/MS results obtained with S9 fractions.

Reduced sensitivity was observed for this type of sample, which was reflected in the relatively short list of metabolites identified in cells, and none in culture medium. Two additional metabolites (M + O and M + SO_3) were identified in cells exposed for 24 h and 48 h (Table 2). Non-metabolized VerA was detected at all exposure times.

Table 2: Compounds detected as $[M-H]^-$ in extracts of IPEC-1 intestinal epithelial cells exposed to VerA for 24 and 48 hours.

Compound	Measured *m/z*	Error (ppm)	Molecular formula	Retention time (min)	Identification level [a]	MS/MS spectrum Observed product ions *m/z* (relative abundance expressed in %)
VerA	337.0348	-1.5	$C_{18}H_{10}O_7$	23.2	1	309.1 (100), 308.1 (55), 293.1 (13), 337.1 (13), 320.1 (5), 265.2 (5), 252.1 (4), 280.1 (3)

M + O *epoxide and/or hydroxylated*	353.0295	-2.3	$C_{18}H_{10}O_8$	18.9	3	309.1 (100), 325.1 (90), 335.2 (69), 281.1 (23), 310.1 (14), 353.4 (10) 265.1 (8), 311.2 (6), 297.2 (6)
M + SO_3	416.9911	-2.4	$C_{18}H_{10}O_{10}S$	22.4	3	337.2 (100), 417.0 (2)

[a] Identification level as defined by Sumner et al., 2007

3.3 VerA metabolites identified in porcine jejunum explants and liver slices

Extracts of liver and jejunum *ex vivo* incubations were analyzed to characterize metabolites of VerA. These models display features close to the *in vivo* situation, including complex tissue architecture and cell diversity. Although still relatively weak, higher sensitivity of the tissues was observed, and a more complete list of metabolites was obtained. Four compounds were identified from tissue samples, all characterized metabolites based on data acquired from human liver S9 incubations, except for one metabolite (M + CH_2) (Table 3). Concerning the sample liver slices, all metabolites were detected in tissue extracts and culture media except the metabolite M + CH_2, which was only detected in liver slices. Only one compound, (M + GlcAc), were detected in the jejunum explant culture medium. Only one epoxide and/or hydroxylated metabolite, (M + O), was found in all tissues from liver origin and cultured cells, whereas the sulfate conjugate (M + SO_3) identified in intestinal cells was not detected in tissues. MS^3 analyses were performed for conjugated metabolites, (M + GlcAc and M + O + GlcAc), to confirm their identification.

Table 3: Compounds detected as $[M-H]^-$ in extracts of porcine jejunum explants and precision-cut liver slices exposed to VerA

Compound	Liver slices samples	Jejunum samples	Liver slices culture media	Jejunum culture media	Measured *m/z*	Error (ppm)	Molecular formula	Retention time (min)	Observed product ions *m/z* (relative abundance)
VerA	Yes	Yes	Yes	Yes	337.0348	-1.5	$C_{18}H_{10}O_7$	23.2	309.1 (100), 308.1 (64), 293.1 (34),337.1 (11)
M + O *epoxide and/or hydroxylated*	Yes	No	Yes	No	353.0303	0	$C_{18}H_{10}O_8$	18.9	325.1 (100), 309.1 (98), 335.2 (94), 281.1 (25),

									310.1 (20), 265.1 (11), 297.1 (9), 353.2 (6), 324.3 (5), 308.2 (5), 307.1 (4)
M + GlcAc	Yes	Yes	Yes	Yes	513.0674	0	$C_{24}H_{18}O_{13}$	19.1	337.1 (100), 513.1 (2), 175.0 (2)
M + O + GlcAc ***epoxide and/or hydroxylated***	Yes	No	Yes	No	529.0624	0	$C_{24}H_{18}O_{14}$	14.2	353.1 (100), 529.1 (2)
M + CH_2	Yes	No	No	No	351.0503	-2.0	$C_{19}H_{13}O_7$	24.9	323.2 (100), 322.2 (54), 351.2 (12), 307.2 (11), 336.2 (6), 266.2 (6), 279.2 (6),

4 Discussion

The toxicity of the bisfuranoid mycotoxins such as AFB1 and its precursor STC largely depends on their biotransformation, which can either lead to the production of less toxic metabolites (detoxification) or of metabolites (or reactive intermediates) that trigger adverse effects following XME-driven bioactivation pathways. One of the pathways involved in the toxicity of mycotoxins is the production of reactive intermediates, which are mutagenic compounds. The balance between bioactivation and detoxification pathways may differ according to the target tissue, depending on the expressed XME. The capability of a given tissue to metabolize mycotoxins into reactive species may define its sensitivity to the adverse effects of these substances. It is therefore essential to characterize the molecules that derive from the metabolization of these mycotoxins. Despite being highly mutagenic and genotoxic, the metabolites of VerA have not been described to date.

The presence of a bisfuran moiety in the structure of VerA and previous literature suggest that one of the biotransformation pathways of this substance could lead to the production of a reactive *exo*-epoxide, as already demonstrated for STC and AFB1 (Díaz Nieto et al., 2018; Rushing and Selim, 2019). In the present study, we provide novel qualitative data concerning VerA, as this is the first study to investigate the metabolization of this molecule.

Since VerA metabolites are not commercially available, our strategy was based on the generation of high quality chromatographic and MS data produced following incubations of large amounts of in-house purified VerA *in vitro* S9 fractions. This strategy was selected so as to produce sufficient amounts of each metabolite in a matrix relatively less complex than biofluids or cell/tissue extracts.

Human S9 fractions are an appropriate well-recognized *in vitro* model to study both phase I and II biotransformation pathways of xenobiotics. Human S9 incubations potentially enable the formation of different metabolites catalyzed by CYP450, flavin-containing monooxygenase (FMOs), UDP-glucuronosyltransferases (UGTs), sulfotransferases (SULTs) and glutathione *S*-transferases (GSTs).With the addition of diverse cofactors, a wider panel of XME activities was investigated than in a previous study (Huber et al., 2021). This approach was then applied to study the VerA metabolism in pigs. Porcine S9 fractions would have been more appropriate to conduct a detailed study of porcine metabolism. However, this protocol was developed to be applied to any xenobiotics in human or any animals after this proof of concept on pigs.

In this study, analytical data were acquired on seven VerA-derived products, including phase I and phase II biotransformation metabolites. Along with the intact toxin, the phase I metabolite M + O compatible with an hydroxylated, but also with an epoxide form of VerA was detected in liver. According to previous data, VerA induces AhR transactivation and the subsequent induction of the expression of the CYP450, enzymes involved in the bioactivation of AFB1 (Budin et al., 2021; Gauthier et al., 2020). VerA up-regulates the expression of multiple CYP450 enzymes in intestinal cells including, CYP1A1, CYP1A2 and CYP3A4 (Gauthier et al., 2020). These three isoforms were previously shown to be involved in the oxidation of AFB1 into the highly mutagenic *exo*-8-9 epoxide (Rendic and Guengerich, 2021) and CYP3A isoforms have been shown to be important in the metabolization of AFB1 in pig (Jiang et al., 2018; Wu et al., 2016). The presence of an epoxide metabolite of VerA is also supported by the high genotoxicity and mutagenicity (Mori et al., 1984; Theumer et al., 2018) that are partially explained by the intense oxidative and replication stress induced by this toxin, leading to double strand DNA breaks (Gauthier et al., 2020; Smela et al., 2002). Although, hydroxylated, endo or exo epoxide structures could not be differentiated from our experimental data, the observed genotoxicity of VerA suggested the production of an exo epoxide metabolite. Further investigations are needed to confirm this

hypothesis, notably the structure of this metabolite by NMR as well as the presence of VerA-DNA or VerA-protein adducts. The epoxide form is usually detoxified into glutathione-conjugated forms mediated by glutathione S-transferases (GSTs), other phase II enzymes (Behrens et al., 2019) and could be consecutively metabolized into other adducts (Hinchman and Ballatori, 1994). The *exo*-AFB1-8-9-epoxyde can be detoxified to a glutathione conjugate by rat and human GSTs (Raney et al., 1992). Regarding the STC, previous experiments using human recombinant CYP1A1 and CYP3A4 enabled the detection of a glutathione conjugate, suggesting the formation of STC-epoxide (Cabaret et al., 2010). Such conjugates were not detected in the present experiment. However, in our experiments, the incubation times of exposed tissues were relatively short. Indeed 24/48 h incubation with VerA enabled the detection of more metabolites than incubation for 3 h in IPEC1 cells. Additional research is warranted to enrich GST-transformed VerA metabolites to overcome possible sensitivity problems. In parallel with epoxide, the M + O metabolite could also represent hydroxylated metabolites. Among four C-positions likely to be hydroxylated, the hydroxylation at C-7 of VerA, which is equivalent to C-9 in STC, could lead to the formation of a catechol. As other possibility, the hydroxylation at C-11 could lead to a hydroxylated metabolite homologous to aflatoxin M1 (Marchese et al., 2018) and 12c-hydroxy-STC (Pfeiffer et al., 2014).

Conjugation pathways (phase II metabolism) are predominantly detoxification processes, leading to more readily excreted metabolites (Kedderis, 2010). Glucuronide metabolites (M + GlcAc and M + O + GlcAc) of VerA produced by UGTs were observed in human liver S9 incubations and in liver. Only the metabolite M + GlcAc was detected in intestinal porcine tissues exposed to the toxin. These results suggest that this probable detoxification pathway are crucial in these organs. This is in line with the known induction of the expression of UGTs by VerA (Gauthier et al., 2020). It has been already shown that glucuronidation, which acts directly on the parent molecule or after hydroxylation, is an important pathway for metabolism of STC and 5-methoxysterigmatocystin (Cabaret et al., 2013, 2011, 2010) and is involved in its urinary and biliary elimination in the vervet monkey (Steyn and Thiel, 1976; Thiel and Steyn, 1973).

Additional sulfate groups were found in human liver S9 incubations (M + SO3 and M + O + SO3) and intestinal porcine epithelial cells (M + SO3). In the porcine tracheal epithelial cells, STC metabolism

resulted in a sulfo-conjugate of hydroxysterigmatocystin (Cabaret et al., 2011), suggesting that sulfonate conjugation may also correspond to a detoxification pathway for VerA. Further studies are needed to investigate the non-toxicity of these conjugated VerA.

5 Conclusion

In the present study, we established the first list of reference metabolites of VerA using human liver S9 fraction incubations coupled with UPLC-HRMS, which we subsequently used to identify VerA metabolites produced in intestinal porcine epithelial cells as well as intestinal and hepatic porcine tissues exposed *ex vivo* to the toxin. Reference metabolites produced *in vitro* were used to produce chromatographic and MS and MS/MS data, thereby improving the identification of VerA metabolites in complex biological matrices. This approach was successfully applied to identify emerging mycotoxins in biological samples from animals, but the same strategy could be used to characterize the exposure of humans to other emerging contaminants. As metabolites corresponding to emerging contaminants of food or of human environments are not currently commercially available, their identification is complex (Bonvallot et al., 2021) and the *in vitro* synthesis of reference metabolites using S9 fractions is a promising approach to improve non-targeted human biomonitoring of xenobiotics.

By this way, a large set of VerA metabolites was characterized that will be useful for further metabolic studies of VerA. A relatively high concentration of VerA was studied to allow the production of this first list of metabolites, which might not be representative of real circulating concentrations. However, no data are now available on these internal concentrations of VerA in exposed animals. The metabolites identified include phase I and phase II metabolites of VerA, thereby revealing potential detoxification pathways (i.e. glucuronidation and sulfation pathways). In addition, we identified a metabolite consistent with the bioactivation of VerA into an epoxide form. If this pathway is confirmed, it could be involved in the genotoxic and mutagenic effects described in the literature for this emerging toxin. The present results warrant further investigation of the metabolism of this dangerous compound, including quantitative measurements of metabolization rates and kinetics of transformations, as well as the detection of VerA-DNA adducts to help explain its high genotoxicity. Taken together, the results of the present study provide analytical data and biological information, which would be valuable to detect

biomarkers of exposure, and biomarkers of effect of VerA useful for the risk assessment of this emerging mycotoxin.

Acknowledgement/Funding

This research was supported in part by the ANR grants "Versitox" (ANR-18-CE21-0009) and "EmergingMyco" (ANR 18-CE34-014), and by CAPES-COFE-CUB under grant SV 947/19.

All LC-HRMS analyses were conducted at MetaToul (Toulouse metabolomics & fluxomics facilities, www.metatoul.fr), which is part of French National Infrastructure MetaboHUB for Metabolomics and Fluxomics [MetaboHUB-ANR-11-INBS-0010] and France Exposome for chemical exposomics. The authors would like to thank Daphne Goodfellow for English editing, and Daniel Zalko (INRAE, Toxalim) for helpful discussions.

459 **References**

460 Allen, F., Pon, A., Wilson, M., Greiner, R., Wishart, D., 2014. CFM-ID : a web server for annotation ,
461 spectrum prediction and metabolite identification from tandem mass spectra. Nucleic Acids Res.
462 12, 94–99. https://doi.org/10.1093/nar/gku436
463 Baertschi, S.W., Raney, K.D., Shimada, T., Harris, T.M., Guengerich, F.P., 1989. Comparison of rates
464 of enzymatic oxidation of aflatoxin B1, aflatoxin G1, and sterigmatocystin and activities of the
465 epoxides in forming guanyl-N7 adducts and inducing different genetic responses. Chem. Res.
466 Toxicol. 2, 114–122. https://doi.org/10.1021/tx00008a008
467 Behrens, K.A., Jania, L.A., Snouwaert, J.N., Nguyen, M., Moy, S.S., Tikunov, A.P., Macdonald, J.M.,
468 Koller, B.H., 2019. Beyond detoxification : Pleiotropic functions of multiple glutathione S-
469 transferase isoforms protect mice against a toxic electrophile. PLoSONE 14, 11: e0225449.
470 https://doi.org/10.1371/journal.pone.0225449
471 Bonvallot, N., Jamin, E.L., Regnaut, L., Chevrier, C., Martin, J., Mercier, F., Cordier, S., Cravedi, J.,
472 Debrauwer, L., Le Bot, B., 2021. Science of the Total Environment Suspect screening and
473 targeted analyses : Two complementary approaches to characterize human exposure to pesticides.
474 Sci. Total Environ. 786, 147499. https://doi.org/10.1016/j.scitotenv.2021.147499
475 Budin, C., Man, H.Y., Al-Ayoubi, C., Puel, S., van Vugt-Lussenburg, B.M.A., Brouwer, A., Oswald,
476 I.P., van der Burg, B., Soler, L., 2021. Versicolorin A enhances the genotoxicity of aflatoxin B1
477 in human liver cells by inducing the transactivation of the Ah-receptor. Food Chem. Toxicol.
478 153, 112258. https://doi.org/10.1016/j.fct.2021.112258
479 Cabaret, O., Puel, O., Botterel, F., Delaforge, M., Bretagne, S., 2013. Metabolic detoxification
480 pathways for 5-methoxy-sterigmatocystin in primary tracheal epithelial cells. Xenobiotica 44, 1–
481 9. https://doi.org/10.3109/00498254.2013.804635
482 Cabaret, O., Puel, O., Botterel, F., Pean, M., Bretagne, S., Delaforge, M., 2011. Contribution of
483 uniformly 13 C - enriched sterigmatocystin to the study of its pulmonary metabolism 25, 2704–
484 2710. https://doi.org/10.1002/rcm.5068
485 Cabaret, O., Puel, O., Botterel, F., Pean, M., Khoufache, K., Costa, J.M., Delaforge, M., Bretagne, S.,
486 2010. Metabolic detoxication pathways for sterigmatocystin in primary tracheal epithelial cells.

487 Chem. Res. Toxicol. 23, 1673–1681. https://doi.org/10.1021/tx100127b
488 Cabaton, N., Zalko, D., Rathahao, E., Canlet, C., Delous, G., Chagnon, M., Cravedi, J., Perdu, E.,
489 2008. Biotransformation of bisphenol F by human and rat liver subcellular fractions. Toxicol.
490 Vitr. 22, 1697–1704. https://doi.org/10.1016/j.tiv.2008.07.004
491 Caceres, I., Al Khoury, A., El Khoury, R., Lorber, S., P. Oswald, I., El Khoury, A., Atoui, A., Puel,
492 O., Bailly, J.-D., 2020. Aflatoxin Biosynthesis and Genetic Regulation: A Review. Toxins. 12,
493 150. https://doi.org/10.3390/toxins12030150
494 Chu, F.S., 2003. MYCOTOXINS | Toxicology. Encycl. Food Sci. Nutr. 4096–4108.
495 https://doi.org/10.1016/b0-12-227055-x/00823-3
496 Cole, R.J., Cox, R.H., 1981. Versicolorin Group, in: Handbook of Toxic Fungal Metabolites.
497 Academic Press, New york, p. 95. https://doi.org/10.1016/B978-0-12-179760-7.50008-5
498 De Graaf, I.A.M., Olinga, P., De Jager, M.H., Merema, M.T., De Kanter, R., Van De Kerkhof, E.G.,
499 Groothuis, G.M.M., 2010. Preparation and incubation of precision-cut liver and intestinal slices
500 for application in drug metabolism and toxicity studies. Nat. Protoc. 5, 1540–1551.
501 https://doi.org/10.1038/nprot.2010.111
502 Díaz Nieto, C.H., Granero, A.M., Zon, M.A., Fernández, H., 2018. Sterigmatocystin: A mycotoxin to
503 be seriously considered. Food Chem. Toxicol. 118, 460–470.
504 https://doi.org/10.1016/j.fct.2018.05.057
505 Eaton, D.L., Beima, K.M., Bammler, T.K., Riley, R.T., Voss, K.A., 2010. Hepatotoxic Mycotoxins.
506 Compr. Toxicol. 9, 527–569.
507 EFSA, 2013. Scientific Opinion on the risk for public and animal health related to the presence of
508 sterigmatocystin in food and feed. EFSA J. 11, 3254. https://doi.org/10.2903/j.efsa.2013.3254
509 European Commission, 2006. Commission Recommendation of 17 August 2006 on the presence of
510 deoxynivalenol, zearalenone, ochratoxin A, T-2 and HT-2 and fumonisins inproducts intended
511 for animal feeding. Off. J. Eur. Union L299, 7–9.
512 European Union, 2006. Commision Regulation (EC) No 1881/2006 of 19 December 2006 setting
513 maximum levels for certain contaminants in foodstuffs. Off. J. Eur. Union 15–16.
514 Fæste, C.K., Ivanova, L., Uhlig, S., 2011. In Vitro Metabolism of the Mycotoxin Enniatin B in

515 Different Species and Cytochrome P450 Enzyme Phenotyping by Chemical Inhibitors. Drug
516 Metab. Dispos. 39, 1768–1776. https://doi.org/10.1124/dmd.111.039529.
517 Gauthier, T., Duarte-Hospital, C., Vignard, J., Boutet-Robinet, E., Sulyok, M., Snini, S.P., Alassane-
518 Kpembi, I., Lippi, Y., Puel, S., Oswald, I.P., Puel, O., 2020. Versicolorin A, a precursor in
519 aflatoxins biosynthesis, is a food contaminant toxic for human intestinal cells. Environ. Int. 137,
520 105568. https://doi.org/10.1016/j.envint.2020.105568
521 Hasuda, A.L., Person, E., Khoshal, A.K., Bruel, S., Puel, S., Oswald, I.P., Bracarense, A.P.F.R.L.,
522 Pinton, P., 2022. Deoxynivalenol induces apoptosis and inflammation in the liver: Analysis using
523 precision-cut liver slices. Food Chem. Toxicol. 163, 112930.
524 https://doi.org/10.1016/j.fct.2022.112930
525 Hendricks, J.D., Sinnhuber, R.O., Wales, J.H., Stack, M.E., Hsieh, D.P.H., 1980.
526 Hepatocarcinogenicity of Sterigmatocystin and Versicolorin A to Rainbow Trout (Salmo
527 Gairdneri) Embryos234. J. Natl. Cancer Inst. 64, 1503–1509.
528 https://doi.org/10.1093/jnci/64.6.1503
529 Hinchman, C.A., Ballatori, N., 1994. Glutathione conjugation and conversion to mercapturic acids can
530 occur as an intrahepatic process. J. Toxicol. Environ. Health 41, 387–409.
531 https://doi.org/10.1080/15287399409531852
532 Huber, C., Muller, E., Schulze, T., Brack, W., Krauss, M., 2021. Improving the Screening Analysis of
533 Pesticide Metabolites in Human Biomonitoring by Combining High-Throughput In Vitro
534 Incubation and Automated LC − HRMS Data Processing. Anal. Chem. 93, 9149–9157.
535 https://doi.org/10.1021/acs.analchem.1c00972
536 International Agency for Research on Cancer (IARC), 1993. Monographs on the Evaluation of
537 Carcinogenic Risks to Humans. IARC Press 56, 245–395.
538 Jacques, C., Jamin, E.L., Perdu, E., Duplan, H., Mavon, A., Zalko, D., Debrauwer, L., 2010.
539 Characterisation of B (a) P metabolites formed in an ex vivo pig skin model using three
540 complementary analytical methods. Anal Bioanal Chem 396, 1691–1701.
541 https://doi.org/10.1007/s00216-009-3389-1
542 Jaeg, J.P., Perdu, E., Dolo, L., Debrauwer, L., Cravedi, J., Zalko, D., 2004. Characterization of New

Bisphenol A Metabolites Produced by CD1 Mice Liver Microsomes and S9 Fractions. J Agric Food Chem 52, 4935–4942. https://doi.org/10.1021/jf049762u

Jakšić, D., Puel, O., Canlet, C., Kopjar, N., Kosalec, I., Klarić, M.S., 2012. Cytotoxicity and genotoxicity of versicolorins and 5- methoxysterigmatocystin in A549 cells. Arch. Toxicol. 86, 1583–1591. https://doi.org/10.1007/s00204-012-0871-x

Jamin, E.L., Bonvallot, N., Tremblay-franco, M., Cravedi, J., Chevrier, C., Cordier, S., Debrauwer, L., 2014. Untargeted profiling of pesticide metabolites by LC – HRMS : an exposomics tool for human exposure evaluation. Anal Bioanal Chem 406, 1149–1161. https://doi.org/10.1007/s00216-013-7136-2

JECFA, 2017. Evaluation of certain contaminants in food, Prepared by the Eighty-third report of the Joint FAO/WHO Expert Committee on Food Additives (JECFA), WHO Technical Report Series. https://doi.org/10.1126/science.1092089

Jiang, H., Wu, J., Zhang, F., Wen, J., Jiang, J., Deng, Y., 2018. The critical role of porcine cytochrome P450 3A46 in the bioactivation of aflatoxin B1. Biochem. Pharmacol. 156, 177–185. https://doi.org/10.1016/j.bcp.2018.08.030

Kawai, K., Nakamaru, T., Hisada, K., Nozawa, Y., Mori, H., 1986. The effects of demethylsterigmatocystin and sterigmatin on ATP synthesis system in mitochondria: A comparison with sterigmatocystin. Mycotoxin Res. 2, 33–38. https://doi.org/10.1007/BF03191960

Kedderis, G.L., 2010. Biotransformation of Toxicants. Compr. Toxicol. 3, 137–151. https://doi.org/10.1016/b978-0-08-046884-6.00107

Lahjouji, T., Bertaccini, A., Neves, M., Puel, S., Oswald, I.P., Soler, L., 2020. Acute Exposure to Zearalenone Disturbs Intestinal Homeostasis by Modulating the Wnt / β -Catenin Signaling Pathway. Toxins. 12, 113. https://doi.org/10.3390/toxins12020113.

Marchese, S., Polo, A., Ariano, A., Velotto, S., Costantini, S., Severino, L., 2018. Aflatoxin B1 and M1: Biological properties and their involvement in cancer development. Toxins. 10, 1–19. https://doi.org/10.3390/toxins10060214

Mori, H., Kawai, K., Ohbayashi, F., Kuniyasu, T., Yamazaki, M., Hamasaki, T., Williams, G.M.,

1984. Genotoxicity of a Variety of Mycotoxins in the Hepatocyte Primary Culture/DMA Repair Test Using Rat and Mouse Hepatocytes1 2918–2923.

Mori, H., Sugie, S., Yoshimi, N., Kitamura, J., Niwa, M., Hamasaki, T., Kawai, K., 1986. Genotoxic effects of a variety of sterigmatocystin-related compounds in the hepatocyte/DNA-repair test and the Salmonella microsome assay. Mutat. Res. Lett. 173, 217–222. https://doi.org/10.1016/0165-7992(86)90039-4

Payros, D., Garofalo, M., Pierron, A., Soler-Vasco, L., Al-Ayoubi, C., Maruo, V.M., Alassane-Kpembi, I., Pinton, P., Oswald, I.P., 2021. Mycotoxins in human food: A challenge for research. Cah. Nutr. Diététique 56, 170–183. https://doi.org/10.1016/J.CND.2021.02.001

Pfeiffer, E., Fleck, S.C., Metzler, M., 2014. Catechol formation: A novel pathway in the metabolism of sterigmatocystin and 11-methoxysterigmatocystin. Chem. Res. Toxicol. 27, 2093–2099. https://doi.org/10.1021/tx500308k

Pinton, P., Nougayrede, J.P., Del Rio, J.C., Moreno, C., Marin, D.E., Ferrier, L., Bracarense, A.P., Kolf-Clauw, M., Oswald, I.P., 2009. The food contaminant deoxynivalenol, decreases intestinal barrier permeability and reduces claudin expression. Toxicol. Appl. Pharmacol. 137, 41–48. https://doi.org/10.1016/j.taap.2009.03.003

Raney, K.D., Meyer, D.J., Ketterer, B., Harris, T.M., Guengerich, F.P., 1992. Glutathione Conjugation of Aflatoxin B1 exo- and endo-Epoxides by Rat and Human Glutathione S-Transferases. Chem. Res. Toxicol 5, 470–478. https://doi.org/10.1021/tx00028a004

Rendic, S.P., Guengerich, F.P., 2021. Human Family 1–4 cytochrome P450 enzymes involved in the metabolic activation of xenobiotic and physiological chemicals: an update. Arch. Toxicol. 95, 395–472. https://doi.org/10.1007/s00204-020-02971-4

Rushing, B.R., Selim, M.I., 2019. Aflatoxin B1: A review on metabolism, toxicity, occurrence in food, occupational exposure, and detoxification methods. Food Chem. Toxicol. 124, 81–100. https://doi.org/10.1016/j.fct.2018.11.047

Schrenk, D., Bignami, M., Bodin, L., Chipman, J.K., del Mazo, J., Grasl-Kraupp, B., Hogstrand, C., Hoogenboom, L., Leblanc, J.C., Nebbia, C.S., Nielsen, E., Ntzani, E., Petersen, A., Sand, S., Schwerdtle, T., Vleminckx, C., Marko, D., Oswald, I.P., Piersma, A., Routledge, M., Schlatter,

599 J., Baert, K., Gergelova, P., Wallace, H., 2020. Scientific opinion – Risk assessment of aflatoxins
600 in food. EFSA J. 18, 112. https://doi.org/10.2903/j.efsa.2020.6040
601 Smela, M.E., Currier, S.S., Bailey, E.A., Essigmann, J.M., 2001. The chemistry and biology of
602 aflatoxin B 1 : from mutational spectrometry to carcinogenesis. Carcinogenesis 22, 535–545.
603 https://doi.org/10.1093/carcin/22.4.535
604 Smela, M.E., Hamm, M.L., Henderson, P.T., Harris, C.M., Harris, T.M., Essigmann, J.M., 2002. The
605 aflatoxin B 1 formamidopyrimidine adduct plays a major role in causing the types of mutations
606 observed in human hepatocellular carcinoma. Natl. Acad. Sci. 99, 6655–6660.
607 https://doi.org/10.1073/pnas.102167699.
608 Staack, R.F., Hopfgartner, G., 2007. New analytical strategies in studying drug metabolism. Anal
609 Bioanal Chem 388, 1365–1380. https://doi.org/10.1007/s00216-007-1367-z
610 Steyn, M., Thiel, P.G., 1976. Biliary excretion of sterigmatocystin by vervet monkeys. Biochem.
611 Pharmacol. 25, 265–266. https://doi.org/10.1016/0006-2952(76)90211-2
612 Sumner, L.W., Amberg, A., Barrett, D., Beale, M.H., Beger, R., Daykin, C.A., Fan, T.W.-M., Fiehn,
613 O., Goodacre, R., Griffin, J.L., Hankemeier, T., Hardy, N., Harnly, J., Higashi, R., Kopka, J.,
614 Lane, A.N., Lindon, J.C., Marriott, P., Nicholls, A.W., Reily, M.D., Thaden, J.J., Viant, M.R.,
615 2007. Proposed minimum reporting standards for chemical analysis Chemical Analysis Working
616 Group (CAWG) Metabolomics Standards Initiative (MSI). Metabolomics 3, 211–221.
617 https://doi.org/10.1007/s11306-007-0082-2.
618 Theumer, M.G., Henneb, Y., Khoury, L., Snini, S.P., Tadrist, S., Canlet, C., Puel, O., Oswald, I.P.,
619 Audebert, M., 2018. Genotoxicity of aflatoxins and their precursors in human cells. Toxicol.
620 Lett. 287, 100–107. https://doi.org/10.1016/j.toxlet.2018.02.007
621 Thiel, P.G., Steyn, M., 1973. Urinary excretion of the mycotoxin, sterigmatocystin by vervet monkeys.
622 Biochem. Pharmacol. 22, 3267–3273. https://doi.org/10.1016/0006-2952(73)90101-9
623 Trail, F., Mahanti, N., Linz, J., 1995. Molecular biology of aflatoxin biosynthesis. Microbiology 141,
624 755–765. https://doi.org/10.1099/13500872-141-4-755
625 US Food and Drugs Administration, 2021. Compliance Policy Guide Sec . 555 . 400 Aflatoxins in
626 Human Food : Guidance for FDA Staff.

US Food and Drugs Administration, 2019. Compliance Policy Guide Sec. 683.100 Action levels for Aflatoxins in animal Food.

Walkow, J., Sullivan, G., Maness, D., Yakatan, G.J., 1985. Sex and Age Differences in the Distribution of 14C-Sterigmatocystin in Immature and Mature Rats: A Multiple Dose Study. J. Am. Coll. Toxicoology 4, 45–51. https://doi.org/10.3109/10915818509014503

Wehner, F.C., Thiel, P.G., van Rensburg, S.J., Demasius, I.P.C., 1978. Mutagenicity to Salmonella typhimurium of some Aspergillus and Penicillium mycotoxins. Mutat. Res. Toxicol. 58, 193–203. https://doi.org/10.1016/0165-1218(78)90009-5

Wong, J.J., Singh, R., Hsieh, D.P.H., 1977. Mutagenicity of fungal metabolites related to aflatoxin biosynthesis. Mutat. Res. Mol. Mech. Mutagen. 44, 447–450. https://doi.org/10.1016/0027-5107(77)90102-6

Wu, J., Chen, R., Zhang, C., Li, K., Xu, W., Wang, L., Chen, Q., Mu, P., Jiang, J., Wen, J., Deng, Y., 2016. Bioactivation and regioselectivity of pig cytochrome P450 3A29 towards aflatoxin B1. Toxins. 8, 1–17. https://doi.org/10.3390/toxins8090267